Environmental Earth Sciences (2018) 77:192
https://doi.org/10.1007/s12665-018-7349-y

ORIGINAL ARTICLE

# A climatology of the annual cycle of river discharges into the Brazilian continental shelves: from seasonal to interannual variability

Julianna Carvalho Oliveira[1,5] · Wilton Aguiar[2] · Mauro Cirano[1,3] · Fernando Genz[4] · Fabiola Negreiros de Amorim[1,3]

Received: 13 January 2017 / Accepted: 18 February 2018 / Published online: 2 March 2018


## Abstract

River runoff into the continental shelf affects the coastal environment in many ways: from sediment input and marine sediments resuspension to meso-scale eddies formation in case of higher river discharges. Therefore, for ocean modeling is crucial to understand the seasonal and interannual river runoff variability. Brazil stands out when it comes to riverine discharge, since 6 out of the 50 largest rivers flows within the country limits. Here, a compilation of all river discharge data provided by the Brazilian National Water Agency resulted in the identification of 97 exorheic rivers (with time series longer than 15 years), including 10 unmonitored ones which had climatologies estimated by the proposed methodology. This compilation took a considerable effort, as streamflow stations were often far from the discharge location. It was also necessary to overcome the challenge associated with the Brazilian climate heterogeneity in order to apply the regionalization method. The riverine input into the ocean was estimated at the mouth of the rivers, with the overall discharge analysis taking into consideration a division of the Brazilian Continental Shelf in five sectors. These results analyzed here are also made available for public use. Overall, the Brazilian northern continental shelf receives about 95% of the total annual river runoff (212,148 $m^3 s^{-1}$), followed by the northeastern continental shelf with 1.5% (3345 $m^3 s^{-1}$), the eastern continental shelf with 1.4% (3097 $m^3 s^{-1}$) and the southern continental shelf with about 1.3% (2997 $m^3 s^{-1}$). The southeastern continental shelf receives only 0.8% of the total discharge (1909 $m^3 s^{-1}$). Throughout the year, the major river discharges were observed from summer to winter months, following the different climate and precipitation patterns along the country. The interannual variability of the discharges was assessed, also looking at similarities regarding both El Niño Southern Oscillation and Pacific Decadal Oscillation.

**Keywords** Brazilian continental shelf · South Atlantic · River discharge · Regionalization · Brazilian rivers

## Introduction

River runoff modifies the circulation and mixing throughout the continental shelf and is the main link between continent and ocean in the hydrological cycle. The discharge of the rivers is important to maintain the salinity balance, flux of sediments and organic matter to the coast, and to create the vertical density gradients, which drives the thermohaline circulation (Oki 1999). In a geological scale, in the ocean, the evaporation exceeds the precipitation, while the opposite occurs at the continent where there is a surplus of precipitation. Therefore, the flow of continental water to the ocean, due to river discharge and groundwater flow, balances the water cycle. This continental freshwater is also the one available for human needs, and its demand increases with the population growth, putting into focus the water management needs, especially in a climate change scenario (Dai et al. 2009).

**Electronic supplementary material** The online version of this article (https://doi.org/10.1007/s12665-018-7349-y) contains supplementary material, which is available to authorized users.

✉ Julianna Carvalho Oliveira
julianna.carvalho@hzg.de

[1] Oceanographic Modeling and Observation Network (REMO), Salvador, Brazil

[2] Federal University of Rio Grande, Rio Grande, Rio Grande do Sul, Brazil

[3] Department of Meteorology, Federal University of Rio de Janeiro, Rio de Janeiro, Rio de Janeiro, Brazil

[4] Department of Environmental Engineering, Federal University of Bahia, Salvador, Bahia, Brazil

[5] Present Address: Helmholtz-Zentrum Geesthacht, Geesthacht, Germany

The coastal region surrounding the mouth of the exorheic system, the main vehicle of continental water to the ocean, can act as a source of momentum, heat and buoyancy to the ocean (Kourafalou et al. 1996). It was demonstrated that the rivers input changes the heat flux, temperature and salinity anomalies, and even coastal current patterns, highlighting that is crucial to account for the river input when studying the coastal ocean circulation (Huang et al. 2010). Examples of alterations caused by specific rivers can also be found on the literature, such as the role of the Congo River on the world oceanic carbon budget (Coynel et al. 2005) and the Mississippi River, where during summer, both the nutrient input and discharge-driven stratification create and hypoxic area of approximately 20,000 $km^2$ (Baumgartner and Reichel 1975).

Since the volume of the discharge is an important variable to understand and predict the coastal circulation and buoyancy, several authors studied the discharge patterns along the world. For instance, Baumgartner and Reichel (1976) were pioneer when estimated the annual continental freshwater discharge using streamflow data from the early 1960s; Perry et al. (1996) calculated the average monthly discharge in further downstream stations of monitored rivers around the world; and Oki et al. (1999) used the precipitation and evaporation budget to estimate the flux of surface continental water to the ocean. The most recent and refined works regarding the spatial and temporal variations of the river input into coastal regions distributed around the world are the ones from Dai and Trenberth (2002) and Dai et al. (2009), in which they combined a database of measured discharge at the furthest downstream station and atmospheric water budget to evaluate the seasonality of the discharge throughout different coastlines. They used modeling to estimate the contribution downstream from the monitoring station, and produced a climatology of discharge with a one degree resolution. Although their results are of a great value for studies regarding the global water budget, for studies of regional numerical modeling of coastal circulation, where refined grids are often adopted, the proposed one-degree climatology could be a rather generalist approach.

River flow forecasting is a prerequisite for many water resources application (e.g., flood warning, reservoir design). However, the complexity of riverine hydrological processes cannot be fully predicted with simple data-driven models. More suitable models account for the highly nonlinear and seasonal river flows, such as artificial neural networks (Wu et al. 2010) and coupled fuzzy-based neural networks (Chau and Wu 2010; Chen et al. 2015). Selecting an adequate set of inputs is a critical step for successful data-driven streamflow prediction. A major obstacle is identifying a reliable set of inputs to model a given hydrological process, as well as the inclusion of irrelevant or redundant inputs hinders the subsequent calibration process (Taormina and Chau 2015). Thus, for regional river flow forecasting, a dataset based on a consistent set of observations can improve and ensure a reliable model output.

Regarding individual continent discharge, Fekete et al. (1999) estimated that the South America is responsible for approximately 30% of the world's river input, and 58% of the total discharge into the Atlantic Ocean. The Amazon River, the biggest world river in both discharge and drainage basin is located on South America, and is responsible for about 18% ($1.8 \times 10^5$ $m^3$ $s^{-1}$) of the global river discharge. This river carries $10^9$ tons of sediment yearly to the coast and has a surface plume that reaches 200 km offshore and 1000 km northwest from its mouth. Although the São Francisco River has typically a small sediment load, the momentum generated on the coast by the river runoff is important because it suspends sediments that will eventually reach the South Equatorial Current (Medeiros et al. 2007). The Doce River has an important role on the sediment delivery for the Brazilian Continental Shelf—hereinafter BCS (Knoppers et al. 1999). In a smaller scale, there are the Jequitinhonha and Paraíba do Sul Rivers, which, despite its magnitude, are also important for the sediment input and buoyancy on the Brazilian Shelf and to maintain large mangrove environments (Bernini and Rezende 2004; Almeida et al. 2007; Souza et al. 2011). In a last scale of discharge is the Paraguaçu River, which even with only 64 $m^3$ $s^{-1}$ of mean discharge is responsible for changes on the tides symmetry and increase in the mean level of high spring tides (Genz et al. 2006; Cirano and Lessa 2007). Assuming that different amount of river discharges have different effects on the coastal ocean circulation, this work aims to describe the river discharge seasonality along the Brazilian coastline in a fine resolution, serving both as basis for small-scale modeling processes, and as a description of the seasonal patterns of discharge on the Brazilian coast.

Considering the complexity of the Brazilian runoff system, the description of its seasonal discharge is a major challenge. This is mainly due to the difficulty in identifying exoreic rivers in this system, because much of the runoff data along the Brazilian shelf is only reliable prior to 2007. However, the effort to construct a river discharge seasonality throughout the Brazilian coastline is an important contribution to regional modeling studies.

In addition, results of the monthly climatology of all river discharges are also included as a complement of this analysis.

## Methodology

### Study area

As a freshwater source, the Brazilian territory is considered the most relevant study area for the Atlantic Ocean, since the Amazon River accounts for about a third of its

freshwater budget (Dai et al. 2009). The Brazilian government, based on a resolution of the National Council of Water Resources, distinguished 12 hydrographic regions in its territory, where nine of them flow into the BCS—Amazon, Tocantins-Araguaia, Parnaíba, Western Northeast, Eastern Northeast, São Francisco, East Atlantic, Southeast Atlantic and South Atlantic—and three of them—Paraguay, Uruguay and Paraná—that form the Río de la Plata estuary located between Argentina and Uruguay.

Climate distribution was analyzed following Köppen classification and further interpretation achieved on Alvares et al. (2013). According to this study, 81.4% of Brazil experiences a *A type* tropical climate, which is found in all hydrographic regions, except for the South Atlantic one. Out of this fraction, 22.6% corresponds to the *Af type*, 27.5% to the *Am type*, 25.8% to the *Aw type* and 5.5% to the *As type*. Semi-arid *BSh type* was found in only 4.9% of the Brazilian territory, typically in the northeast region. Finally, 13.7% of the Brazilian territory corresponds to the subtropical climate types, where the *Cfa* zone is the most relevant, found in 6.7% of the territory.

The BCS is inserted into a passive continental margin and its shape and width vary considerably along its extent. It reaches its maximum width in the Amazon mouth surroundings (330 km), from where it decreases eastwards and reaches its narrowest width in the vicinity of Salvador and Ilhéus (5–8 km) (Dominguez et al. 2009). Southwards from this point, the average width increases due to the Río de la Plata influence, achieving a wider continental shelf (~ 100 km) (Martins and Coutinho 1981).

A few divisions of the Brazilian continental shelf and coastal zones exist using parameters such as physiographic characteristics (e.g., Martins and Coutinho 1981) and productivity (e.g., Ekau and Knoppers 1999). The subdivision of the BCS adopted in this study was proposed by Knoppers et al. (1999). This classification considers both geological and geographical aspects, as well as the climate and tidal regimes, drainage basin areas, shelf width, length of coastline and coastal current systems. We believe that those factors affect directly the river discharge and the freshwater interactions over the shelf.

Knoppers et al. (1999) created five major divisions for the BCS: (1) North region (4°N–3°S, Northern Shelf Sector—NSS); (2) Northeast region (3°S–13°S, Northeastern Shelf Sector—NESS); (3) East region (13°S–22°S, Eastern Shelf Sector—ESS); (4) Southeast region (22°S–29°S, Southeastern Shelf Sector—SESS) and (5) South region (29°S–34°S, Southern Shelf Sector—SSS).

## Data

The main streamflow data ($m^3\ s^{-1}$) source for this study was the HidroWeb database created by the Brazilian National Water Agency (ANA). The HidroWeb database presents the most updated streamflow measurements within the Brazilian territory and hence was chosen to be used in this study. Exorheic watersheds, as well as the farthest downstream station of each watershed and information on the total drainage area, were identified using shape files of each hydrographic region, available in two different resolutions: a 1:250,000 scale and a finer resolution with 1:100,000, used for smaller watersheds. Number of gaps and record length (≥ 15 years) were considered in the screening section for streamflow time series acquisition (Kennard et al. 2010). In addition, a maximum length of 30 more recent years of data was attributed, in order to adjust for major human interventions such as the 1950–1980 active period of damming in Brazil (Genz 2006). Tributary rivers were not solely analyzed, but included as part of a major watershed. Thus, streamflow data from any tributaries located after the main station were also taken into account.

River streamflow measurements are usually done at some distance from the river mouth, and hence, estimation of loss or addition of water volume on unmonitored areas is necessary in order to estimate the real amount of freshwater discharging over the shelf. Several methods are used to approximate the river flow to its conditions downstream, such as estimation of evaporation and precipitation, water cycle models and statistical models. Although the use of the balance between precipitation and evaporation (P–E) to estimate the river runoff is a rather straightforward method, limitations in this method arise from lack of precipitation measurements, or uncertainties in estimates of P–E by atmospheric reanalysis. Also, in reanalysis, there are documented biases in moisture convergence and atmospheric circulation, which can alter the P–E balance and result in erroneous streamflow values (Trenberth et al. 2001a, b). The modeling approach faces similar problems as the methods using the P–E balance, because water cycle models are forced by the measurements and atmospheric reanalysis estimates of P–E, and hence, the aforementioned biases tend to propagate into the streamflow calculations. As an example, Dai and Trenberth (2002) after estimating the global runoff using the River Transport Model (RTM), attribute the biases in their estimates to errors in Atmospheric reanalysis values of P–E and also to the lack of precipitation data. Finally, even though statistical models such as the one applied in our manuscript do not consider directly precipitation and evaporation, they use the relationship between the previous time series of streamflow and climate conditions to derive the streamflow of ungauged areas. Hence, the use of statistical models has the advantage to use real monitored data, to estimate the streamflow downstream, eliminating the uncertainties related to lack of precipitation data, and erroneous circulation in atmospheric reanalysis.

Two statistical methods were proposed in order to estimate the streamflow at the mouth of each watershed: the regionalization approach and the drainage-area ratio method. The regionalization approach is understood as a difficult task in hydrological science, requiring individual and detailed analyses whenever applied, since there is no universal method (Sivapalan et al. 2003). It consists of transferring information in a homogeneous region, from some location to another, due to similarities in terms of runoff response to specific characteristics such as climate, geology and vegetation (Razavi et al. 2013). For this study, the approach consisted of an adaptation of Dai and Trenberth (2002) Eq. (1) to principles of regionalization proposed by Tucci (2002):

$$Q_{(j)} = Q_{o(j)}\left[1 + r_{(j)}\frac{A_{u(j)}}{A_{m(j)}}\right] \quad (1)$$

where $Q_{(j)}$ is the streamflow at the watershed mouth; $Q_{o(j)}$ is the streamflow at the station; $A_{u(j)}$ is the unmonitored drainage area; $A_{m(j)}$ is the area covered by the monitoring station; and $j$ index stands for a specific month. The ratio $r_{(j)}$ corresponds to the regionalization correction and is the major adjustment to Dai and Trenberth (2002) equation. Dai and Trenberth (2002) successfully used the Eq. (1) to add the streamflow of ungauged areas to the river discharge estimate, using $r_{(j)}$ as the ratio of runoff over unmonitored and monitored areas derived from the Community Land Model, version 3 (CLM3). Validation within the previous study showed that the equation efficiently reproduced the runoff of major global rivers, with some uncertainties related to the biases in the balance between precipitation and evaporation used to derive the river runoff ratio ($r_{(j)}$) in the model products used. Hence, in order to derive better runoff values, we chose to change the sources for calculations of the $r_{(j)}$ ratios. Here, instead, a regression model was developed for each month of a particular homogeneous region, and $r_{(j)}$ could be calculated as:

$$r_{(j)} = \frac{Q'_{(j)} - Q'_{o(j)}}{Q_{o(j)}} \quad (2)$$

where $Q'_{(j)}$ is the monthly streamflow at the watershed mouth derived from its specific regression model when given its total catchment area ($A_m + A_u$), and $Q_o{}'_{(j)}$ is the monthly streamflow at the station estimated by the regression model if given $A_m$. Thus, by using climatological monthly means derived from the main station of each watershed, as well as their monitored catchment area, it was possible to estimate the ungauged area contribution and, therefore, to calculate the runoff climatology. A sensitivity test to evaluate whether a region was homogeneous or not was accomplished through regression analysis and coefficients of determination ($R^2$), where the independent variable was the gauged catchment area ($A_m$) and the dependent one was the mean streamflow at the mouth ($Q'_{(j)}$).

An advantage of using the linear regression to evaluate homogeneity instead of direct evaluation of climatic parameters of each watershed is the simplicity of the application of this method, which requires the two variables mentioned above. As a general rule, priority was given to coefficients of which the proportion of variance for the dependent variable could be explained by the independent variable, i.e., the streamflow, in the order of 70% or above ($R^2 > 0.70$). This approach is especially easy to use, because it requires only the catchment area and the streamflow measurement ($A_m$ and $Q'_{(j)}$). A limitation of the method happens when values of $R^2$ lower than 0.70 occur, due to heterogeneity of watershed. In order to surpass this limitation, we decided then to construct more than one regression model by sector, when $R^2 < 0.70$.

An alternative method adopted was the drainage-area ratio method (Hirsch 1979), which was used in the following cases: (1) the absence of homogeneity in the established region, given by small coefficients of determination ($R^2 < 0.70$) and (2) the monitored area is smaller than 30% of the total drainage area. In these cases, the method consists of estimating the discharge by using the proportion between total drainage area and monitored area:

$$Q = Q_o\frac{A_t}{A_m} \quad (3)$$

where $A_t$ is the total catchment area. We chose the drainage-area ratio method because, similarly to the regionalization, it uses the areas of monitored and unmonitored streamflow, and hence has similar results. This method presumes that the whole extension of the river is homogeneous and subject to the same hydrological conditions; therefore, a linear proportion is applied in order to estimate the discharge at the mouth. A limitation on this approach is that, since the total area is always bigger than the monitored one, final discharge at river mouth will be necessarily higher then monitored discharge. This is only a problem in watersheds with extremely dry conditions downstream, so we did not apply the drainage-area method in those situations. Finally, although the homogeneity of river flow is a limitation of both methods, the analysis of the homogeneity of the river throughout its extension is a viable way to fix this flaw, diminishing methodology errors.

## Interannual variability and El Niño Southern Oscillation—ENSO

In order to evaluate the interannual variability of the river discharge over the BCS, anomalies of streamflow were

calculated following Pekárová et al. (2006) and Genz and Luz (2012):

$$\text{Anomaly} = \frac{(Q_i - Q_m)}{\sigma} \quad (4)$$

where $Q_i$ is the annual average streamflow ($m^3\ s^{-1}$) for a given year $i$, $Q_m$ is the mean annual streamflow ($m^3\ s^{-1}$), and $\sigma$ is the standard deviation ($m^3\ s^{-1}$). The calculation of anomalies according to Genz and Luz (2012) converts the streamflow into a dimensional, similarly to the process used to calculate climate indexes such as Southern Ocean Oscillation and Nino3.4. We believe those characteristics contribute to a more reliable analysis of interannual variability, and hence, this normalization approach was used.

Dai et al. (2009) concluded that ENSO events were correlated to annual and decadal variability in river discharge in the Atlantic, Pacific and Indian oceans, due to the precipitation anomalies normally driven by the El Niño and La Niña phases. In order to evaluate this relationship, the anomalies were compared to the Southern Oscillation Index (SOI), calculated by the Australian Bureau of Meteorology following the Troup SOI method and available at http://www.bom.gov.au/climate/current/soihtm1.shtml (Vaz et al. 2006; Barros and Marques 2012). This index gives an indication of the development and intensity of the phenomena in the Pacific Ocean, where sustained negative values of the SOI greater than − 8 often suggests El Niño episodes, whereas sustained positive values of the SOI greater than + 8 are typical of a La Niña episode.

Several other ENSO indices are commonly used to understand the discharge variability due to interannual cycles (e.g., Niño-4, Niño-3.4 or JMA). However, the majority of studies on the BCS use the SOI index to understand the interannual variability of the associated discharge, and it was chosen here for consistency.

## Results and discussion

A total of 97 exorheic watersheds were identified, and 38 were selected as the most relevant in terms of mean monthly discharge. Among the 97 exorheic watersheds, 10 of them show no monitoring stations and had monthly discharge values estimated here (S1 Table). Table 1 gathers the basic information of the selected rivers, and Fig. 1 shows the location of the associated rivers. This section is organized in two main parts. The first part focuses on the seasonal variability of the discharges, following the proposed BCS classification. The second section discusses the discharge interannual variability, in terms of the ENSO and Pacific Decadal Oscillation (PDO) climatic modes.

Indexes were chosen based on the river mouth locations, from West to East for rivers in the NSS and from North to South for the other sectors. The stations used for each watershed are represented by its denomination at the ANA database, and the river mouth locations are given by latitude and longitude coordinates. A complete Table with all the 97 rivers analyzed in this work is presented in S1 Table, in the form of a spreadsheet.

### Seasonal variability

#### Northern Shelf Sector (NSS)

This is the most important shelf sector when it comes to understanding and assessing the runoff influence, since the Amazon and Tocantins mouths are located in its surroundings. It is a region of diverse climate regimes, including 4 Köppen climate types—*Am, As, Aw, Af* and *BSh*—and riverine influence from the Amazon, Tocantins-Araguaia, Parnaíba, Western Northeast and Eastern Northeast hydrographic regions. It receives a mean annual riverine discharge of 212,148 $m^3\ s^{-1}$, with April presenting the peak discharge of 306,932 $m^3\ s^{-1}$ and November showing the minimum discharge of 118,015 $m^3\ s^{-1}$. This study identified 27 watersheds that flow into the NSS, with seven of them being selected as more relevant, as shown in Fig. 2. Among the 27 watersheds identified, 9 were unmonitored, accounting for an area of 24,413 $km^2$ which were then included in the estimation of the discharge for the NSS.

With exception of the Amazon, Tocantins and Parnaíba watersheds, due to their huge extension, the Araguari River, which had a unique streamflow to drainage area relationship, and the Moju River, which had only 12% of monitored drainage area, all other rivers from the NSS had their discharge estimated following the regionalization approach. Two different regions were created in the NSS in order to apply this methodology, which were called East and West divisions. The latter included all rivers to the left of the Mearim River, while the former covered the rest of them, including the Mearim River. Coefficients of determination for the linear approximation of the East division varied between 0.91 (June) and 0.99 (January), whereas for the West division the results were slightly lower, varying between 0.87 (December) and 0.97 (April). Therefore, in both cases, the drainage area was able to predict the river discharge in more than 87%. Climatology of these regions was remarkably different, with the East being more similar to the NESS. For the rivers which skipped this approach, the streamflow data at the mouth were estimated following the area proportion method. Estimation of runoff values for the Amazon watershed followed Dai et al. (2009) and consisted of summing up data from its main station (Óbidos—17050001) with the tributary rivers which entered the main stream below it.

**Table 1** Characteristics of the main Brazilian rivers flowing into the associated continental shelves presented in Fig. 1

| Index | River | Stations (ANA) | Total drainage area ($km^2$) | Latitude (°) | Longitude (°) | Start year | Final year | Mean annual discharge ($m^3\ s^{-1}$) |
|---|---|---|---|---|---|---|---|---|
| 1 | Amazon | 17050001 | 6,112,000 | − 0.75 | − 51.75 | 1976 | 2005 | 193,573 |
| | | 17730000 | | | | 1987 | 2007 | |
| | | 17090000 | | | | 1974 | 2005 | |
| | | 18300000 | | | | 1973 | 1989 | |
| | | 19150000 | | | | 1977 | 2007 | |
| | | 18850000 | | | | 1977 | 2006 | |
| | | 19985000 | | | | 1981 | 2005 | |
| 2 | Caciporé | 30060000 | 5694 | 4.01 | − 51.46 | 1984 | 1994 | 218 |
| | | 30055000 | | | | 1996 | 2005 | |
| 5 | Araguari | 30400000 | 37,078 | 1.27 | − 49.83 | 1977 | 2006 | 1146 |
| 6 | Tocantins | 29700000 | 786,738 | − 1.75 | − 49.25 | 1978 | 2006 | 12,081 |
| 7 | Moju | 31020000 | 29,483 | − 1.55 | − 48.51 | 1982 | 2005 | 2730 |
| 8 | Guamá-Capim | 31700000 | 50,186 | − 1.45 | − 48.51 | 1971 | 2006 | 696 |
| | | 31520000 | | | | 1976 | 2006 | |
| 14 | Gurupi | 32620000 | 35,204 | − 1.15 | − 46.16 | 1976 | 2006 | 465 |
| 17 | Mearim | 33190000 | 97,988 | − 3.13 | − 44.66 | 1975 | 2005 | 437 |
| | | 33380000 | | | | 1974 | 2007 | |
| | | 33290000 | | | | 1975 | 2005 | |
| 24 | Parnaíba | 34879500 | 333,606 | − 2.74 | − 41.80 | 1982 | 2005 | 862 |
| | | 34980000 | | | | 1976 | 2005 | |
| 29 | Jaguaribe | 36390000 | 74,128 | − 4.50 | − 37.76 | 1975 | 2005 | 85.1 |
| | | 36580000 | | | | 1975 | 2005 | |
| 32 | Piranhas-Açu | 37710150 | 40,848 | − 5.10 | − 36.61 | 1985 | 2006 | 87.2 |
| 39 | Paraíba | 38895000 | 19,752 | − 7.08 | − 34.83 | 1970 | 1997 | 27.4 |
| 44 | Una | 39560000 | 6427 | − 8.80 | − 35.09 | 1977 | 2006 | 36.5 |
| 48 | São Francisco | 49705000 | 644,806 | − 10.54 | − 36.35 | 1977 | 2007 | 2729 |
| 57 | Paraguaçu | 51350000 | 54,463 | − 12.84 | − 38.79 | 1975 | 2005 | 89.8 |
| 58 | Jaguaripe | 51560000 | 2686 | − 13.14 | − 38.80 | 1975 | 2005 | 25.6 |
| 59 | Jequirica | 51685000 | 7069 | − 13.22 | − 38.92 | 1975 | 2006 | 13.1 |
| 60 | Das almas | 51890000 | 3092 | − 13.37 | − 38.94 | 1975 | 2005 | 33.7 |
| 63 | De contas | 52831000 | 56,414 | − 14.27 | − 38.99 | 1976 | 2006 | 101 |
| | | 52830000 | | | | 1976 | 2006 | |
| 65 | Pardo | 53950000 | 32,466 | − 15.63 | − 38.94 | 1969 | 2005 | 71.7 |
| 67 | Jequitinhonha | 54950000 | 72,710 | − 15.84 | − 38.88 | 1975 | 2005 | 420 |
| 69 | Jucuruçú | 55340000 | 6420 | − 17.34 | − 39.22 | 1975 | 2005 | 77.3 |
| 70 | Alcobaça | 55490000 | 7022 | − 17.53 | − 39.20 | 1971 | 2005 | 46.8 |
| 72 | Mucuri | 55740000 | 16,310 | − 18.10 | − 39.55 | 1971 | 2006 | 102 |
| 73 | São Mateus | 55960000 | 13,428 | − 18.71 | − 39.74 | 1975 | 2005 | 81.4 |
| 74 | Doce | 56998000 | 90,030 | − 19.65 | − 39.81 | 1967 | 1994 | 983 |
| 76 | Itapemirim | 57580000 | 6498 | − 21.00 | − 40.81 | 1981 | 2012 | 90.3 |
| 77 | Itabapoana | 57930000 | 5316 | − 21.30 | − 40.96 | 1975 | 2005 | 66.3 |
| 78 | Paraíba do Sul | 58974000 | 64,079 | − 21.64 | − 41.08 | 1975 | 2005 | 761 |
| 84 | Ribeira do Iguape | 81683000 | 27,575 | − 24.66 | − 47.41 | 1971 | 2001 | 498 |
| 86 | Itapocu | 82770000 | 3199 | − 26.60 | − 48.67 | 1977 | 2006 | 135 |
| | | 82350000 | | | | 1977 | 2006 | |
| 87 | Itajaí | 83870000 | 16,846 | − 26.89 | − 48.63 | 1989 | 2006 | 507 |
| | | 83900000 | | | | 1968 | 2006 | |
| 88 | Tijucas | 84095500 | 2517 | − 27.23 | − 48.61 | 1964 | 1983 | 57.2 |

**Table 1** (continued)

| Index | River | Stations (ANA) | Total drainage area ($km^2$) | Latitude (°) | Longitude (°) | Start year | Final year | Mean annual discharge ($m^3\ s^{-1}$) |
|---|---|---|---|---|---|---|---|---|
| 90 | Tubarão | 84580500 | 4902 | − 28.54 | − 48.76 | 1991 | 2004 | 192 |
| 91 | Araranguá | 84820000 | 2449 | − 28.93 | − 49.35 | 1977 | 2006 | 74.9 |
| | | 84949800 | | | | 1978 | 2007 | |
| | | 84853000 | | | | 1977 | 2004 | |
| 94 | Jacuí | 87382000 | 92,560 | − 30.30 | − 51.19 | 1973 | 2005 | 2000 |
| | | 85900000 | | | | 1977 | 2006 | |
| | | 87170000 | | | | 1974 | 2005 | |
| | | 86720000 | | | | 1983 | 2006 | |
| 95 | Camaquã | 87905000 | 16,765 | − 31.27 | − 51.62 | 1977 | 2007 | 367 |
| 97 | Piratini | 88680000 | 24,688 | − 32.01 | − 52.42 | 1962 | 1983 | 441 |

The last data entry was between the years of 2005 and 2007, with the time series length of about 30 years for the majority of streamflow stations, except for the Caeté and Caciporé Rivers with only 15 years of data. Caciporé streamflow data were submitted to concatenation between two streamflow stations: 30060000 and 30055000, since they were only 12 km apart and their time span was complementary to each other. Total drainage area consisted of 7,644,665 $km^2$, where 91.49% were monitored by the ANA, 8.29% was estimated in this study and 0.17%, corresponding to four rivers with a short time series length accounting for 12,920 $km^2$, was excluded from the methodology.

As presented in Fig. 2, the riverine discharges for NSS are higher in the first semester of the year, as a result of the characteristics of the leading tropical climate regime. This feature is especially notable for the eastern rivers, closer to the NESS, where, except for the Parnaíba River, the monthly discharges are lower than 100 $m^3\ s^{-1}$ during drier periods (June to December). Seasonality shows a clear trend of higher discharges from March to May, with the majority of rivers having a peak during April. Also, it is easy to notice a strong decline during April and June, as a result of lower rainfall. This coupling between rainy season and the strongest streamflow months is only possible because the Amazon River, which has the highest discharge value, is classified as only moderately affected by damming. Furthermore, damming along the course of the NSS is a critical issue, since the watersheds of the exorheic rivers cover more than eight biomes in South America, increasing the environmental sensitivity due to runoff regularization (Nilsson et al. 2005).

The Amazon watershed reaches the maximum discharge in May, and minimum in November. The average discharge ranges from 111,104 to 273,666 $m^3\ s^{-1}$. It is observed that the flood season occurs later in relation to the distribution of rainfall. This may be a result of the bimodal rainfall regime or due to the contribution of subsurface drainage (Zeng 1999). According to Silva et al. (2005), the freshwater inflow from the Amazon River corresponds to 18% of continental freshwater released into the oceans and its sediment plume can reach up to 200 km offshore, even affecting the North Equatorial Countercurrent and contributing to eddies formation (Johns et al. 1990).

The Tocantins River, the second most relevant riverine input, shows the highest streamflow from January to April, with a peak in March. This is slightly sooner than the nearby rivers, given that the rainy season is from December to February. The size of its drainage area (786,738 $km^2$) is the feature that supports the delay of one month at the maximum flow rate relative to the maximum precipitation (Costa et al. 2003). Its estimated historical discharge was 11,738 $m^3\ s^{-1}$.

The Araguari River presents one of the most peculiar climatologies from all rivers which flow into the NSS. Besides having a larger period of increased streamflow as a result of a less sharp decrease during the austral winter, its streamflow versus drainage area is superior when compared to rivers from the same sector. Its historical average streamflow is 1146 $m^3\ s^{-1}$ over < 30,000 $km^2$, while other rivers with the same streamflow magnitude, such as Parnaíba, present about ten times larger areas in order to account for such high discharges. When it comes to the Parnaíba River, the peak flow in April (2126 $m^3\ s^{-1}$) corresponds to the concentration of rainfall in the first 4 months of the year, which is also the flood season and presents higher values of standard deviation (not shown). According to ANA (2005), the Parnaíba River has an average annual flow of 776 $m^3\ s^{-1}$ (compared to 862 $m^3\ s^{-1}$ calculated in this work) and corresponds to the smallest flow rate when compared to the other 12 hydrographic regions defined by the National Council of Water Resources.

### Northeastern Shelf Sector (NESS)

This region experiences large seasonal variation in riverine input, derived mainly from the Eastern Northeast and São

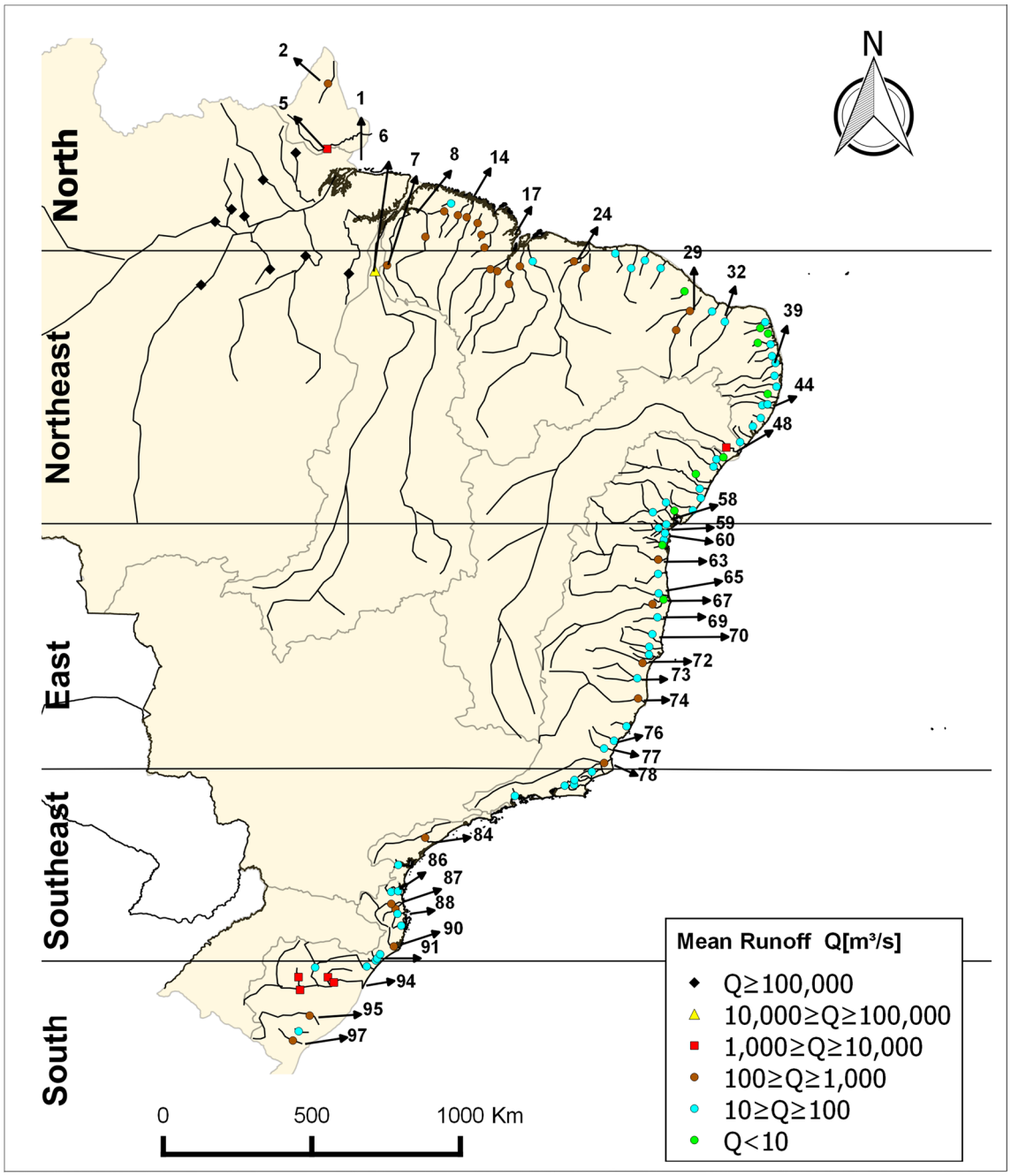


**Fig. 1** Map showing the stations and watersheds used in the study. Symbols and colors were chosen to represent specific discharge ($Q$) intervals

Francisco hydrographic regions, including some portion of the East Atlantic region. The existence of ephemeral rivers is not rare, due to the presence of semi-arid climate (*BSh*). The mean annual discharge for this sector is 3345 $m^3\ s^{-1}$, and the climatology shows a minimum runoff in October (2518 $m^3\ s^{-1}$) and a peak in April (4641 $m^3\ s^{-1}$). The most relevant river is the São Francisco, which flows into the ocean between Sergipe and Alagoas states, accounting for about 82% of the riverine input in this sector. This is the third most important riverine discharge in Brazil (Dai and Trenberth 2002), showing a peak discharge in February (3882 $m^3\ s^{-1}$) and a minimum in July (2121 $m^3\ s^{-1}$). There are 28 exorheic watersheds, of which the most relevant ones are named in Fig. 3. The time series are all very recent (final year between 2005 and 2009), except for the Paraíba River (final year in 1997), with time span ranging from 18 to 30 years of data.

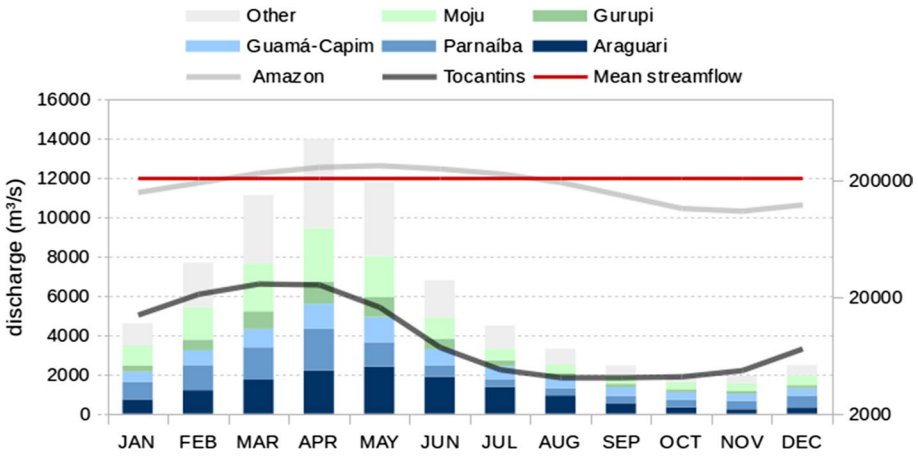


**Fig. 2** Climatology of the monthly riverine discharge into the NSS. The secondary *Y* axis is logarithmic and has the purpose of representing the Amazon and Tocantins Rivers, which have an order of magnitude larger than the remaining rivers. The mean discharge (in red) is also associated with the secondary axis. The geographical location of each watershed as well as the relevant information associated with each main watershed is presented in Fig. 1 and Table 1, respectively. A spreadsheet with a full description of all the watershed analyzed is available in S1 Table

The total drainage area is 937,016 km$^2$, with 94% being monitored by the ANA and 6% corresponding to the area between the most downstream station and the river mouth, which were estimated in this study.

Although the seasonality of the derived runoff of the NESS seems quite similar in shape to the NSS, the unique seasonal behavior of each watershed made it very difficult to apply the regionalization method, as a consequence of the interaction between the different Köppen climate types in the region—*BSh, As, Am* and *Aw*—as well as due to the existence of many intermittent rivers. According to Nilsson et al. (2005), the NESS is formed of rivers both moderately and strongly affected by dam construction, which can show a peculiar climatology when compared to rivers of the same climatic type. They also show that runoff regulation through damming has the strongest impact over the southern half of the NESS.

As a result, three different groups were created in order to best estimate the discharge for each river following the regionalization approach. Overall, rivers in the same group were geographically located nearby, which highlights the role of climate in determining the seasonal variation in the streamflow. The northernmost division included seven watersheds, which were highly subject to a semi-arid climate and, as a consequence, the best fit for this data was the logarithmic approximation, with coefficients of determination ranging from 0.71 to 0.94. A second division covered seven rivers, mostly from about 8°S and 10°S, resulting in a linear approximation with $R^2$ values ranging from 0.71 to 0.86. The southernmost division included five rivers primarily influenced by the *Aw* climate type, which presents drier winter seasons. The best fit for this division was also linear with the $R^2$ values ranging from 0.68 in July to 0.98 in February. Although July and August showed coefficients of determination slightly lower than the ideal minimum threshold of

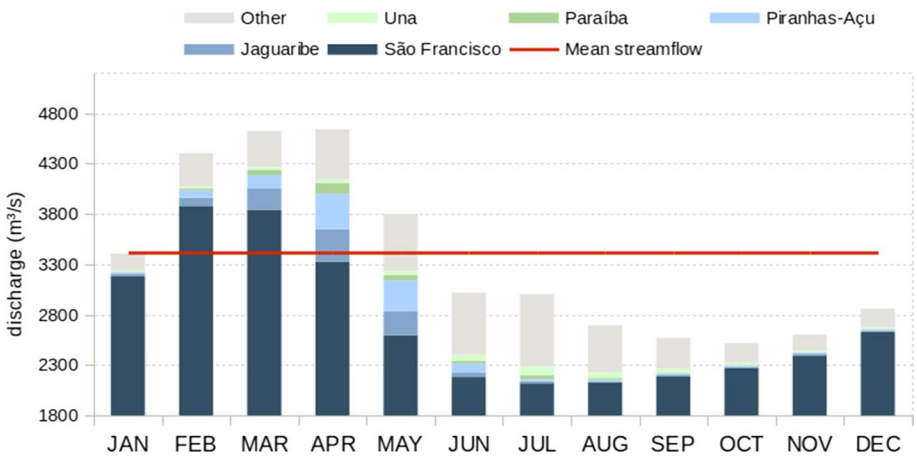


**Fig. 3** Climatology of the monthly riverine discharge into the NESS. The geographical location of each watershed as well as the relevant information associated with each main watershed are presented in Fig. 1 and Table 1, respectively. A spreadsheet with a full description of all the watershed analyzed is available in S1 Table

0.70, this was expected since drier conditions may lead to complicated data sets when streamflow values tend to zero and, ultimately, suggests that high evaporation rates may be responsible for this behavior. The last NESS river subject to the regionalization approach was the Curu River, which had its discharge estimated according to the East division from NSS due to its proximity. Finally, the last eight rivers which flow into the NESS followed the area proportion method, since it was not possible to adjust their data to none of the regional divisions.

Paraíba River reaches its maximum streamflow in April (105.4 $m^3 s^{-1}$) and, after decreasing during May and June, shows a second peak in July (41.9 $m^3 s^{-1}$). This behavior represents the transition between rainfall patterns for Ceará and Alagoas states (ANA 2005). High values of standard deviation from February to May are due to the drainage basin response to heavy rains and the predominance of superficial runoff, as a result of a low permeable soil (not shown). This is also a characteristic of other semi-arid rivers such as the Piranhas-Açu.

Jaguaribe River shows a similar climatology to rivers from the NSS. It is the largest river from the Brazilian semi-arid region and the main source of water for the state of Ceará. Since 1990 this river has undergone major changes, especially due to the Castanhão reservoir activity which has fundamentally controlled its regime and decreased its streamflow variation (Frota et al. 2013).

Lastly, Una River shows a peculiar climatology, presenting a higher streamflow in winter. Drier season occurs from August to February (30–100 mm/month), while the wetter months include March to July (120–210 mm/month) (ANA 2005).

#### Eastern Shelf Sector (ESS)

This region presents a narrow shelf and receives low sediment input from the coast, due to the resistant rocks of the Barreiras formation (Lacerda et al. 1993). In contrast, some of the rivers with low sediment input still account for the sedimentation rate on the shelf, i.e., Jequitinhonha and Doce Rivers (Smoak and Patchineelam 1999). Five Köppen climate types can be found in the ESS: *Af*, *Am*, *Aw*, *Bsh* and *BWh*. This great diversity can be seen from the coast to inland, where the conditions vary from the *Af* Wet tropical Rainforest to the *BWh* desertic type (MMA 2006a). This causes changes in the seasonal regime and hydrological potential of large watersheds. While small coastal watersheds have a high hydrological potential because they are located at the super-humid *Af* climate area, large rivers reach the inland desertic climate region, and as a consequence, their hydrological potential is smaller. A clear example of that is the Paraguaçú River, which has the highest drainage area of the rivers inside the Eastern Shelf Region, but its runoff is not as high as one would expect because great part of its watershed is inside the *BWh* and *BSh* climate types. Finally, as the downstream area of a river tends generally to be smaller than the upstream area, one would expect the river seasonality to answer more accurately to the upstream climatic conditions. This change in hydrological response from coast to inland is present only in the uppermost part of the eastern shelf, since the southern part seems to be entirely at the super-humid climate zone.

Considering the differences in the ESS seasonal regimes and the climatic gradient in the northern part of the shelf, the eastern shelf was divided in three main homogeneous areas to apply the regionalization method. The first homogeneous region hosts the rivers to the south of the Jequitinhonha watershed, from 17.7°S to 22°S. This region has a tropical monsoon climate (*Am*), being humid throughout the whole year. North of 17.7°S, the rivers were divided in homogeneous regions according to their size, i.e., the watersheds with areas larger than 2900 $km^2$ represent one homogeneous region, and the ones with area lower than that represents a second region. It was necessary because smaller watershed discharges respond mainly to the super-humid weather conditions, while the larger ones have their runoff controlled also by dry conditions upstream.

Using the proposed method, 23 exorheic watersheds were found, with the Contas River being monitored by two gauging stations. Those two stations are 700 m distant, and for the regionalization, they were considered the same, due to their complementary time series. After the regionalization, we achieved a coverage area of the ESS watersheds of about 89.2%, corresponding to 458,859 $km^2$, from where 3171 $km^2$ were excluded from the methodology and 409,645 $km^2$ were under monitoring by the ANA. The northernmost homogeneous region containing the watersheds with larger areas is constituted by the rivers Paraguaçú, de Contas, Pardo, Jequiriçá, Cachoeira e Peruípe, while the southernmost homogeneous area hosts the watersheds with more humid conditions—Salsa, Subaé, Jaguaripe and Jequié Rivers. The regionalization process was performed respecting these limits of homogeneous regions.

High determination coefficient values were obtained for all regions, ranging from 0.80 to 0.97. The southernmost area showed the smallest determination coefficient values, ranging from 0.74 in November until 0.92 in March. This is expected since the gradient of precipitation is not a homogeneous feature and furthermore increases the variability.

Figure 4 shows the climatological cycle of the rivers discharge in ESS, after the regionalization. It is clear in the graph that the main tributaries of the ESS are the Doce, Paraíba do Sul and Jequitinhonha Rivers, with mean annual discharge values of 983, 761 and 420 $m^3 s^{-1}$, respectively, representing 68% of the total discharge in into the ESS. For instance, during summer, the Doce River can release more

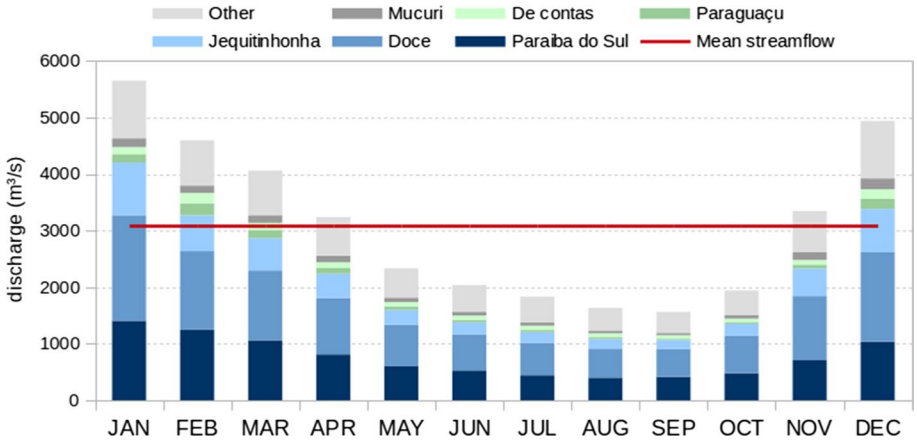


**Fig. 4** Climatology of the monthly riverine discharge into the ESS. The geographical location of each watershed as well as the relevant information associated with each main watershed is presented in Fig. 1 and Table 1, respectively. A spreadsheet with a full description of all the watershed analyzed is available in S1 Table

than 1800 $m^3\ s^{-1}$, according to the regionalization method. The other rivers in the region have mean annual discharge values lower than 200 $m^3\ s^{-1}$. The Paraguaçu, de Contas and Mucurí Rivers together with the main ones represent the six major rivers in the ESS, being responsible for 78% of the total shelf discharge. It is important to highlight that differently from Knoppers et al. (1999), the Paraguaçú River seems to have an important role in the local discharge pattern, being the sixth largest river in discharge. However, the fact that Paraguaçú River had the vastest unmonitored area inserts some uncertainty in the measurement.

The climatological cycle shows a clear drought period during the austral winter, while the peak of discharge occurs during the austral summer, which presents lower precipitation values as described for the drainage area of Paraiba do Sul, Doce, São Mateus, Itapemirim and Itabapoana Rivers (Marengo and Alves 2005). The maximum total discharge into the shelf as estimated by the method is 5649 $m^3\ s^{-1}$ during January, when it starts to decrease until reaching 1561 $m^3\ s^{-1}$ in September. This intense pattern in the discharge shows the strong seasonality inherent to the region, and the importance to take into account the seasonal variation when modeling the coastal circulation of the ESS.

The mean annual discharge into the shelf was 3097 $m^3\ s^{-1}$, which is lower than the value of 3600 $m^3\ s^{-1}$ found by Knoppers et al. (1999). This difference expresses the increasing urban and agricultural pressure on the water resources, and the regularization of discharge by the increasing damming (Souza et al. 2011). The database released by Dai and Trenberth (2002) has a higher value of mean discharge for EES of approximately 3646 $m^3\ s^{-1}$, which can be explained by the fact that the approximation based on the balance between precipitation and evaporation used by the authors do not take into account the impact of the agricultural and urban land usage in diminishing the discharge downstream. In fact, the southernmost area of the EES is classified by Nilson et al. (2005) as strongly affected by flow regulation due to dam construction. Changes in land coverage can, for instance, increase the runoff response to precipitation, and conversion from forest to agriculture may increase the streamflow (Saurral et al. 2008). Those factors change the soil permeability, and estimations of discharge using the balance between evaporation and transpiration can be misleading.

Also, the majority of the stations used in the last study had measurements only until 1999.

### Southeastern Shelf Sector (SESS)

This region is adjacent to the Santa Catarina, Paraná and São Paulo states, and south of Rio de Janeiro. It corresponds to the second smallest sector in the Knoppers et al. (1999) classification. Due to the presence of the Serra do Mar mountain ranges, this region is characterized by a reduced outflow into the ocean. Overall, 14 watersheds and 18 stations were selected, mostly included in the South Atlantic hydrographic region. The Köppen climate classification for this region is *Cfa* (closer to the coastline) or *Cfb* (inner catchment), which means an oceanic climate with absence of a dry season and a hot or mild summer, respectively. The lack of a dry season results in a very smooth variation in the climatology of the SESS. Also, the SESS and SSS are the South American regions with the strongest impacts on runoff due to damming, which contributes to a smoother seasonal cycle (Nilsson et al. 2005). The average annual discharge for this sector is 1909 $m^3\ s^{-1}$ and the climatology (Fig. 5) shows minimum runoff in August (1453 $m^3\ s^{-1}$) and maximum in February (2686 $m^3\ s^{-1}$) as a response for the increased austral summer precipitation found in the region. According to Grimm et al. (1998), the region's relief is the likely cause for the summer's wet season peak, since it is likely to enhance the temperature contrast at the land-sea interface.

The total drainage area relative to the SESS is 70,402 $km^2$, of which 64.5% (45,397 $km^2$) was monitored by ANA and the other 35.5% was estimated in this study. Streamflow estimation at the mouth of each watershed was accomplished

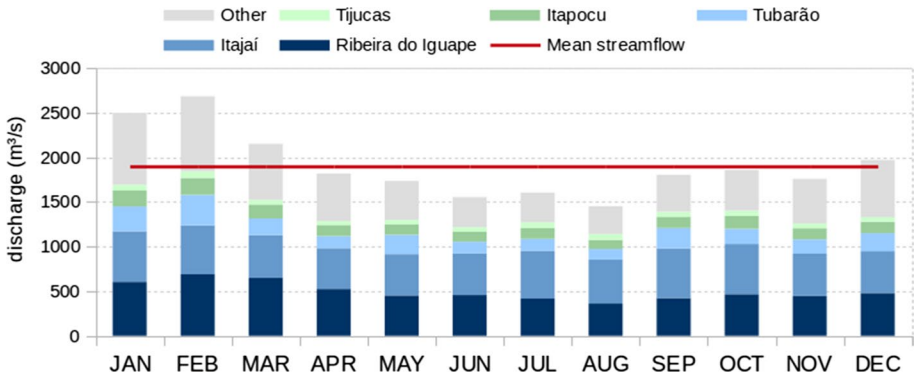


**Fig. 5** Climatology of the monthly riverine discharge into the SESS. The geographical location of each watershed as well as the relevant information associated with each main watershed is presented in Fig. 1 and Table 1, respectively. A spreadsheet with a full description of all the watershed analyzed is available in S1 Table

following the proposed regionalization method. The linear approximation was chosen as the best fit and coefficients of determination ranged from 0.71 in January to 0.98 in March, showing that the model was suitable for predicting most of the discharge in function of the drainage basin. The most relevant rivers in terms of average discharge are Itajaí (507 $m^3\ s^{-1}$), Ribeira do Iguape (498 $m^3\ s^{-1}$), Tubarão (192 $m^3\ s^{-1}$) and Itapocu (135 $m^3\ s^{-1}$). All other ten watersheds showed annual streamflow below 100 $m^3\ s^{-1}$.

The Itajaí River, the largest river in the SESS, showed a maximum discharge in January (567 $m^3\ s^{-1}$), followed by a second peak in October (563 $m^3\ s^{-1}$) and a minimum in April (460 $m^3\ s^{-1}$). This small variation in the annual climatology is a common behavior for rivers in the SESS. The precipitation pattern seems to be followed by the discharge climatology, since the months with higher precipitation are January (170 mm), February (195 mm) and October (166 mm), according to data from the pluviometric station Indaial (MMA 2006b).

For Ribeira do Iguape, the second largest river in the SESS, the maximum streamflow during summer is explained by the rainfall distribution in the region, which is more pronounced from October to March. Registro station, the largest one for this watershed, is also characterized by the highest frequency of floods especially during summer, which can also be suggested by looking at the high standard deviation values for these months: 429 ± 122 $m^3\ s^{-1}$ (December), 542 ± 172 $m^3\ s^{-1}$ (January), 622 ± 170 $m^3\ s^{-1}$ (February) (not shown).

The Tubarão River showed a similar behavior, with maximum discharge in February (345 $m^3\ s^{-1}$) and minimum in August (120 $m^3\ s^{-1}$). According to data from Rio do Pouso pluviometric station, months with higher precipitation are January to March (141–173 mm), which seems to explain the peak discharge season for this river. An interesting feature observed in this river is the susceptibility to flooding events (Marques 2010), which could be observed by calculating the standard deviation values for the 84580500 station (not shown).

### Southern Shelf Sector (SSS)

This region represents the smallest sector, corresponding generally as the coastline of Rio Grande do Sul state. The runoff derived from Brazilian rivers and affecting this region is formed by the watersheds of the Jacuí, Camaquã, Piratini and Arroio Pelotas Rivers, in addition to one unmonitored river which had the streamflow estimated (index 93 in S1 Table). Although not entirely Brazilian, the Paraná and Uruguai hydrographic regions, which flow into the Río de la Plata estuary in Argentina, have a major influence in the SSS (Barros and Marques 2012; Möller et al. 2010) and its annual cycle was investigated in detail by Berbery and Barros (2004). Its total drainage area corresponds to 141,798 $km^2$, from which 60.2% was monitored by the ANA and 38.8% was estimated in this study.

Estimation of streamflow at the mouth, i.e., at the Patos/Mirim lagoon surroundings, was possible through the regionalization approach. A linear regression performed a good fit of the data, where for all months at least 99% of the resulting discharge was due to the drainage basin characteristics. Through those regressions it was also possible to predict the climatology from the unmonitored river described above. Overall, the mean discharge estimated by this method for the SSS was 2997 $m^3\ s^{-1}$, varying from a minimum discharge of 1464 $m^3\ s^{-1}$ in mid austral summer (January) to a maximum of 4888 $m^3\ s^{-1}$ in July (Fig. 6). Higher values were obtained by using the alternative area proportion method, with an average discharge of 3317 $m^3\ s^{-1}$ (7.03% higher), a peak in July of 5354 $m^3\ s^{-1}$ (9.29% higher) and a minimum 1781 $m^3\ s^{-1}$ in January (21.67% higher). Although the reliability of using the regionalization approach may be questionable since the number of rivers in the SSS is small, by choosing this methodology it was possible to increase the monitored area by 4% in the region, due to the estimation of discharge for river 93.

The SSS discharge climatology is different from the SESS, despite their proximity, since the former presents a very notable discharge peak during the austral winter due to increased precipitation as a response to frontal penetration

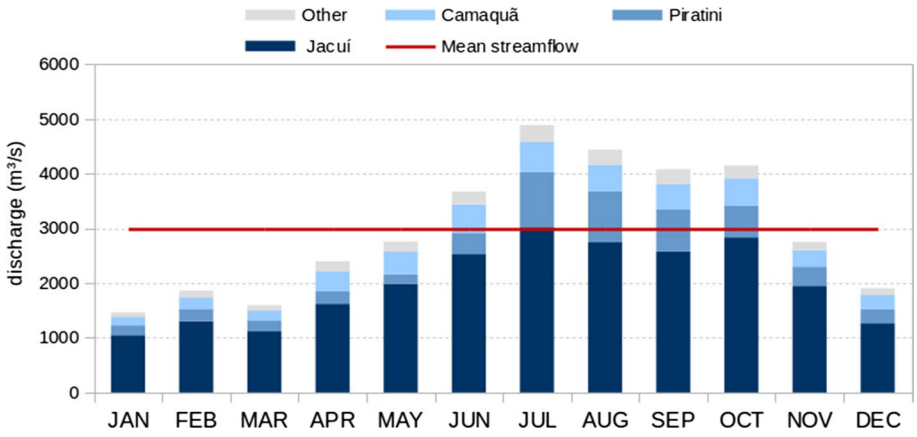


**Fig. 6** Climatology of the monthly riverine discharge for the SSS. The geographical location of each watershed as well as the relevant information associated with each main watershed is presented in Fig. 1 and Table 1, respectively. A spreadsheet with a full description of all the watershed analyzed is available in S1 Table

associated with migratory extratropical cyclones (Grimm et al. 1998), and low temperatures typical from the subtropical climate. Even though this shelf region is considered as strongly regulated by dams, the seasonal cycle of the extratropical cyclone was still enough to input a seasonal variation in the discharge (Nilson et al. 2005). The Jacuí watershed, which includes the tributaries Caí, Dos Sinos and Taquari, consists in the major freshwater source to the Patos/Mirim lagoon complex (Möller et al. 2001), accounting for 65% of the riverine outflow. The Camaquã and Piratini Rivers, on the other hand, are responsible for 11 and 17%, respectively.

### Interannual variability

In order to investigate the overall trend in interannual variability, streamflow anomalies were calculated and cross-correlated to the ENSO index, SOI and also to the PDO index. Cross-correlation values for lag zero varied from low to moderate positive or negative correlation, with no clear trends, except for the NSS and SSS sectors. For the NSS sector, SOI was positively correlated to the anomalies, with values varying from 0.03 for the Tocantins River and 0.44 for Capim-Guamã River, whereas correlation values between anomalies and PDO showed a negative correlation varying from − 0.11 (Parnaíba River) to − 0.53 (Araguari River). This result corroborates with Marengo (1992), which states that a warm phase of the ENSO (El Niño) normally is followed by a decrease in the precipitation of the north of Brazil, with consequently negative streamflow anomalies. Espinoza et al. (2009) analyzed the Amazon basin discharge fluctuations and concluded that the first mode of variability of most associated rivers is controlled by ENSO phases. According to Foley et al. (2002), higher correlations for the Amazon and Tocantins Rivers with the SOI have a 6 months lag, associated with the delayed response of precipitation anomalies over the North of Brazil due to ENSO, as well as due to the residence time of runoff in the region's soil (Zeng 1999).

The moderate negative correlation calculated for the Araguari River also corroborates the findings of Marengo et al. (1998), which mentions that its discharge reflects the interannual changes associated with the extremes of the Southern Oscillation, and especially the strong El Niño events of 1982–1983 and 1992 years (Fig. 7a).

The NESS is expected to follow the same relationship between precipitation and ENSO phase as the NSS Rivers (Marengo et al. 1998), although Fig. 7b shows a tendency to drier conditions in the region, especially from the late 1980s. This trend is likely due to extensive agricultural irrigation or to the activity of hydropower plants, mainly in the case of São Francisco River. In an assessment of the hydrological regime in the downstream part of the São Francisco River, Genz and Luz (2012) showed that the operation of the dams was responsible for 59% of the hydrological changes, while the climate (in driest conditions) has contributed to 41% of the total changes. Cross-correlation values were too small for both SOI and PDO (highest value $p = 0.24$, for the Piranhas-Açu River), which was also the case for the ESS ($p$ varying from − 0.22 to − 0.09). For the ESS (Fig. 7c), its main River Paraíba do Sul seems to follow the same trend as the SESS (Fig. 7d), with El Niño phases normally preceding positive streamflow anomalies (Ovalle et al. 2013). For instance, very wet conditions (streamflow positive anomaly of about 1.5), according to Genz and Luz (2012) classification, were found in the 1982–1983 El Niño.

SESS and SSS (Fig. 7e) present an opposite behavior when compared to the north of Brazil: for instance, El Niño events are normally followed by increasing precipitation and consequently positive streamflow anomalies. Cross-correlation values for lag zero showed moderate values (− 0.36 to − 0.42) when testing the relationship between SOI and discharge anomalies for the SSS, and weak values (− 0.10 to − 0.34) for the SESS. The link between ENSO and river discharge in these regions has been largely studied due to the occurrence of several floods (e.g. Grimm et al. 1998, 2000; Vaz et al. 2006; Barros and Marques 2012; Isla and Toldo

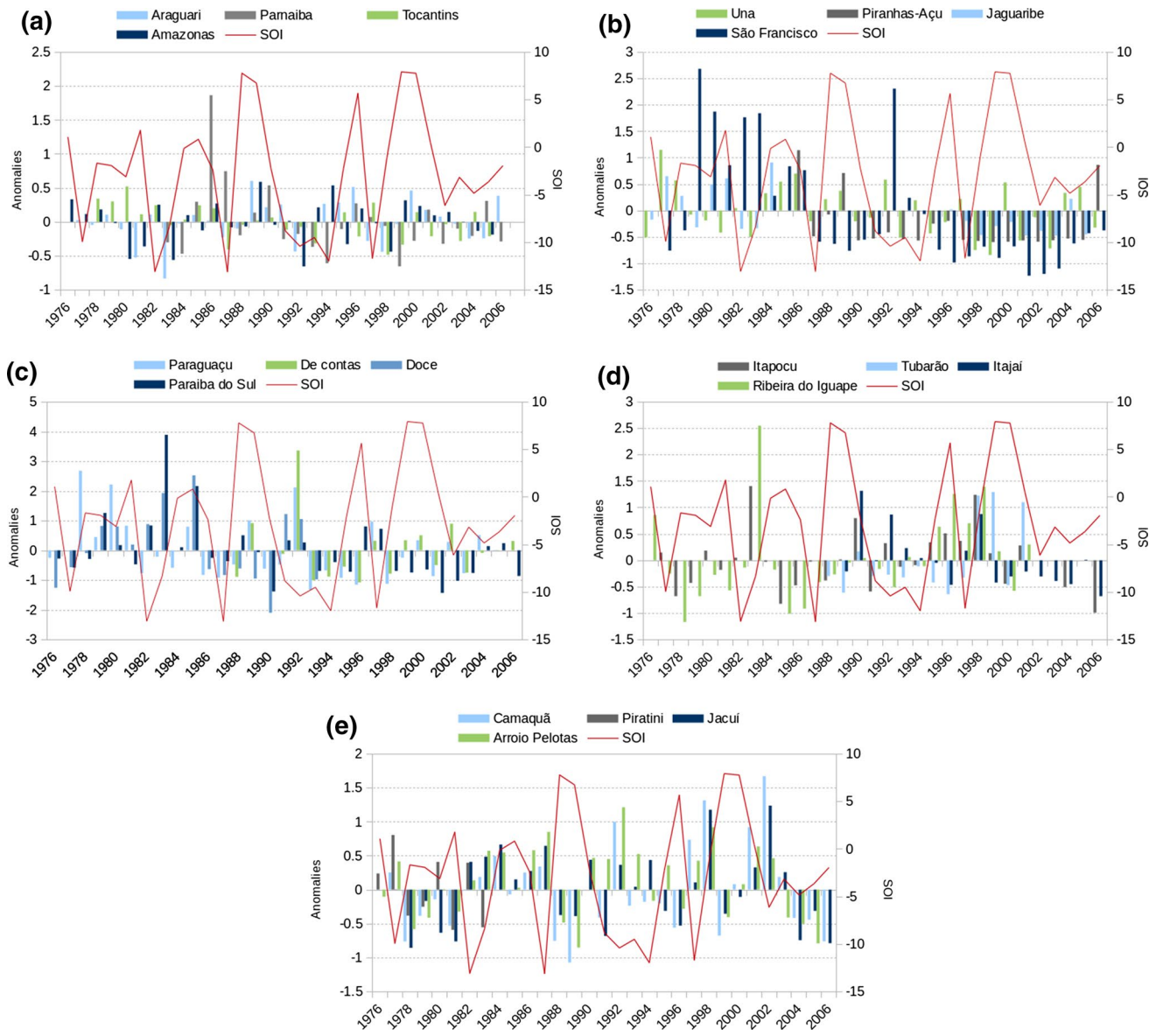


**Fig. 7** Time series of the normalized anomalies of the annual discharge for the main stations of each sector. **a** Amazon, Tocantins, Araguari and Parnaíba Rivers (from NSS); **b** São Francisco, Piranhas-Açu, Jaguaribe and Una Rivers (from NESS); **c** Paraguaçu, De Contas, Doce and Paraíba do Sul Rivers (from ESS); **d** Itapocu, Ribeira do Iguape, Tubarão and Itajaí Rivers (from SESS); **e** Jacuí, Camaquã, Piratini and Arroio Pelotas Rivers (from SSS). The SOI index is indicated by the right *y* axis

Junior 2013), with the incoming freshwater discharge to the Patos Lagoon influenced by the ENSO with a 3.8–6 years cycle.

## Summary and conclusions

The riverine discharges along the Brazilian coast present a wide range of forcing mechanisms, with the potential of exerting different impacts on the BCS. The major discharge is found in the NSS, representing 95% of the total mean annual discharge, followed by 1.5% for the NESS, 1.4% for the ESS, 1.3% for the SSS and lastly 0.8% for the SESS. It is relevant to highlight that for the NSS, NESS and SSS only one specific river accounted for more than 65% of its overall discharge (Amazon, São Francisco and Jacuí Rivers, respectively). The input of each sector is summarized in Fig. 8, where the NSS showed the highest mean annual discharge, with a value of 212,148 $m^3 s^{-1}$, followed by NESS, ESS, SSS and SESS, where the annual discharges are two orders of magnitude lower than the first one.

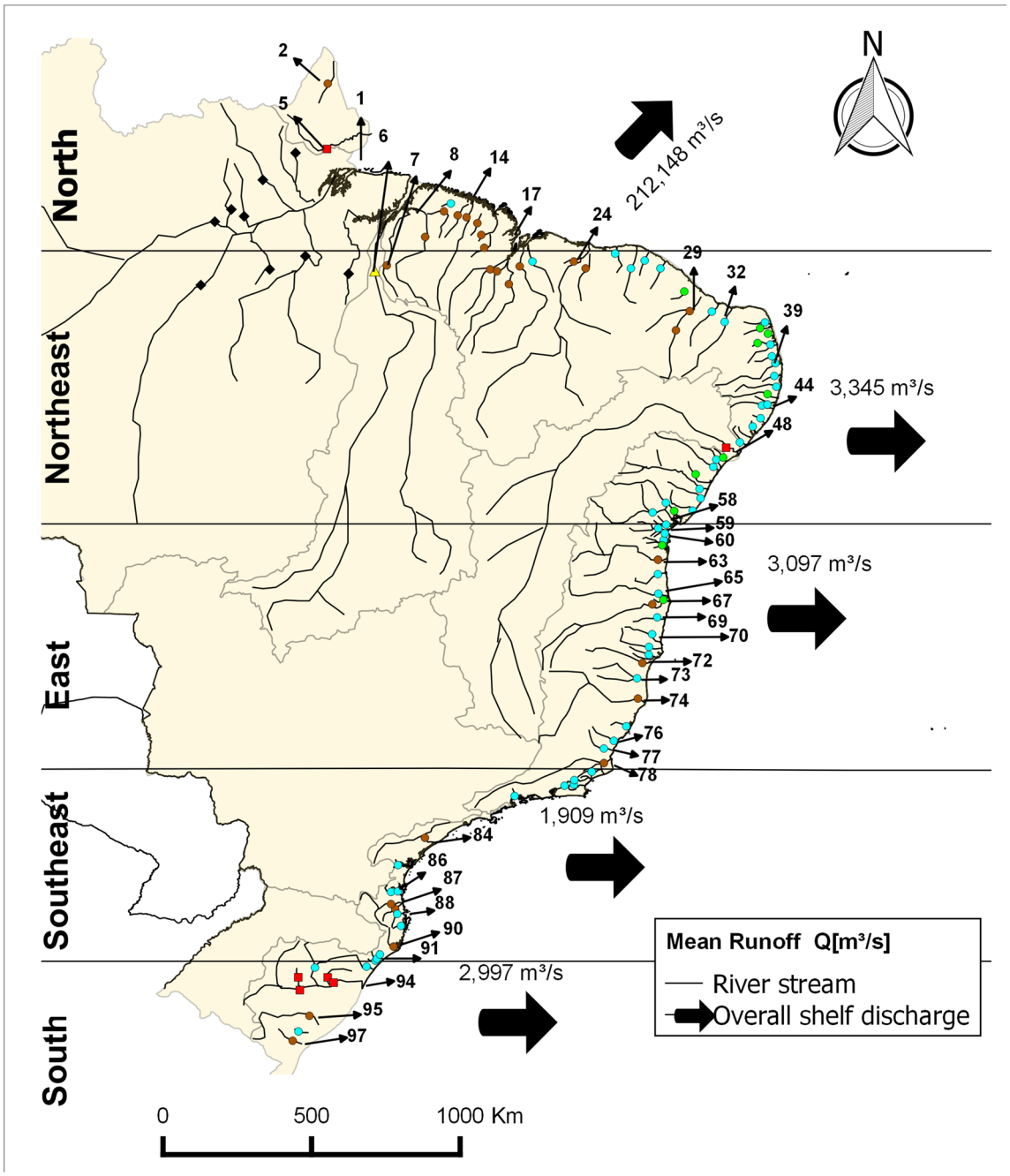


**Fig. 8** Summary of riverine inputs along the BCS

This study pioneered the estimation of discharge for Brazilian rivers using in situ streamflow measurements, providing more reliability for riverine data to be used in coastal modeling, for instance. Using streamflow data for an interval of minimum 15 years and maximum 30 years of more recent records of the Brazilian National Water Agency (ANA), it was possible to apply a regionalization technique for estimating the discharge at the mouth of each exorheic river, instead of relying on values given by monitoring stations often positioned far from the ocean. The study also provided an increase in the monitored area covered by each shelf sector, from north to south, of: 8.3, 6.0, 10.7, 35.5 and 38.8%, respectively. Major developments were shown in southern regions, where the monitoring was less remarkable. The evaluation of discharges in sectors of the continental shelf was also innovating, showing a clear variation in terms of discharge following the climate of the hydrographic regions associated with each region, with wetter conditions varying

from summer to winter months. This was also useful to better estimate the streamflow at the mouth of each watershed, where the regionalization approach was used.

Interannual variability related to SOI and PDO did not show a clear trend within specific sectors, except for the NSS (SSS) sectors, which showed only positive (negative) correlation values between SOI and the streamflow anomalies, and negative (positive) correlation between PDO and the streamflow anomalies. For the other sectors, the lack of significant correlation might be related to anthropogenic activities such as damming, but it could also be associated with the role of the Atlantic sea surface temperature and atmospheric circulation in the riverine outflows. Thus, correct conclusions on the role of climatic modes on the variability of the river discharges require further knowledge on the impact of those installations on each watershed.

Finally, this is a first general study focusing on the estimation of discharges over the BCS and its associated annual variability. For a more thorough investigation, we recommend that next studies could focus on single regions of the shelf. Inclusion of other variables on the discharge model such as soil use and groundwater influence, as well as the use of satellite measurements, is also imperative to the next estimates of the discharge over the BCS. In conclusion, we believe the estimates produced by this study are valuable, especially for enhancing the accuracy of the discharges in models of continental shelf circulation.

**Acknowledgements** This research was supported by PETROBRAS and approved by the Brazilian oil regulatory agency ANP (Agência Nacional de Petróleo, G as Natural e Biocombustíveis), under the special participation Oceanographic Modeling and Observation Network (REMO) research project. M. Cirano and F. N. Amorim were supported by Brazilian scholarships from the Brazilian Research Council (CNPq).

## References

Almeida MG, Rezende CE, Souza CMM (2007) Variação temporal, transporte e partição de Hg e carbono orgânico nas frações particulada e dissolvida da coluna d'água da Bacia Inferior do rio Paraíba do Sul, RJ, Brasil. Geochimica Brasiliensis 21(1):111–129

Alvares CA, Stape JL, Sentelhas PC, Moraes JL, Sparovek G (2013) Köppen's climate classification map for Brazil. Meteorol Z 22(6):711–728. https://doi.org/10.1127/0941-2948/2013/0507

Barros GP, Marques WC (2012) Long-term temporal variability of the freshwater discharge and water levels at Patos Lagoon, Rio Grande do Sul, Brazil. Int J Geophys. https://doi.org/10.1155/2012/459497

Baumgartner A, Reichel E (1975) The world water balance: mean annual global, continental and maritime precipitation and runoff. Elsevier, New York

Berbery EH, Barros VR (2002) The hydrologic cycle of the La Plata Basin in South America. J Hydrometeorol 3(6):630–645. https://doi.org/10.1175/1525-7541(2002)003<0630:THCOTL>2.0.CO;2

Bernini E, Rezende CE (2004) Estrutura da vegetação em florestas de mangue do estuário do rio Paraíba do Sul, Estado do Rio de Janeiro, Brasil. Acta Bot Bras 18(3):491–502. https://doi.org/10.1590/S0102-33062004000300009

Chau KW, Wu CL (2010) A hybrid model coupled with singular spectrum analysis for daily rainfall prediction. J Hydroinform 12(4):458–473. https://doi.org/10.2166/hydro.2010.032

Chen XY, Chau KW, Busari AO (2015) A comparative study of population-based optimization algorithms for downstream river flow forecasting by a hybrid neural network model. Eng Appl Artif Intell 46(A):258–268. https://doi.org/10.1016/j.engappai.2015.09.010

Cirano M, Lessa GC (2007) Oceanographic characteristics of Baía de Todos os Santos, Brazil. Revista Brasileira de Geofísica 25(4):363–387. https://doi.org/10.1590/S0102-261X2007000400002

Costa MH, Botta A, Cardille JA (2003) Effects of large-scale changes in land cover on the discharge of the Tocantins River, Southeastern Amazonia. J Hydrol 283(1–4):206–217. https://doi.org/10.1016/S0022-1694(03)00267-1

Coynel A, Seyler P, Etcheber H, Meybeck M, Orange D (2005) Spatial and seasonal dynamics of total suspended sediment and organic carbon species in the Congo River. Glob Biogeochem Cy 19(4):GB4019. https://doi.org/10.1029/2004gb002335

Dai A, Trenberth KE (2002) Estimates of freshwater discharge from continents: latitudinal and seasonal variations. J Hydrometeor 3(6):660–687. https://doi.org/10.1175/1525-7541(2002)003<0660:EOFDFC>2.0.CO;2

Dai A, Qian T, Trenberth KE, Milliman JD (2009) Changes in continental freshwater discharge from 1948 to 2004. J Clim 22(10):2773–2792. https://doi.org/10.1175/2008JCLI2592.1

Dominguez JML (2009) The coastal zone of Brazil. In: Dillenburg SF, Hesp PA (eds) Geology and geomorphology of holocene coastal barriers of Brazil. Springer, New York, pp 17–52

Dortch Q, Whitledge TE (1992) Does nitrogen or silicon limit phytoplankton production in the Mississippi River plume and nearby regions? Cont Shelf Res 12(11):1293–1309. https://doi.org/10.1016/0278-4343(92)90065-R

Ekau W, Knoppers B (1999) An introduction to the pelagic system of the north-east and east Brazilian shelf. Arch Fish Mar Res 47:113–132

Espinoza JC, Guyot JL, Ronchail J, Cochonneau G, Filizola N, Fraizy P, Labat D, de Oliveira E, Ordoñez JJ, Vauchel P (2009) Contrasting regional discharge evolutions in the Amazon basin (1974–2004). J Hydrol 375(3–4):297–311. https://doi.org/10.1016/j.jhydrol.2009.03.004

Fekete BM, Vorosmarty CJ, Grabs W (1999) Global, composite runoff fields based on observed river discharge and simulated water balances. Tech Rep 22, Global Runoff Data Cent, Koblenz, Germany. http://www.bafg.de/GRDC/EN/02_srvcs/24_rprtsrs/report_22.pdf?__blob=publicationFile

Foley JA, Botta A, Coe MT, Costa MH (2002) El Niño-Southern oscillation and the climate, ecosystems and rivers of Amazonia. Glob Biogeochem Cy 16(4):79-1–79-20. https://doi.org/10.1029/2002gb001872

Frota FF, Paiva BP, Schettini CA (2013) Intra-tidal variation of stratification in a semi-arid estuary under the impact of flow regulation. Braz J Oceanogr 61(1):23–33. https://doi.org/10.1590/S1679-87592013000100003

Genz F (2006) Avaliação dos efeitos da barragem Pedra do Cavalo sobre a circulação estuarina do rio Paraguaçu e Baía de Iguape. Ph.D. Thesis. Federal University of Bahia

Genz F, Luz LD (2012) Distinguishing the effects of climate on discharge in a tropical river highly impacted by large dams. Hydrol Sci J 57(5):1020–1034. https://doi.org/10.1080/02626667.2012.690880

Grimm AM, Ferraz SET, Gomes J (1998) Precipitation anomalies in Southern Brazil associated with El Niño and La Niña

events. J Climate 11:2863–2880. https://doi.org/10.1175/1520-0442(1998)011<2863:PAISBA>2.0.CO;2
Grimm AM, Barros VR, Doyle ME (2000) Climate variability in Southern South America associated with "El Niño" and "La Niña" events. J Climate 13(1):35–58. https://doi.org/10.1175/1520-0442(2000)013<0035:CVISSA>2.0.CO;2
Hirsch RM (1979) An evaluation of some record reconstruction techniques. Water Resour Res 15(6):1781–1790. https://doi.org/10.1029/WR015i006p01781
Huang B, Mehta VM (2010) Influences of freshwater from major rivers on global ocean circulation and temperatures in the MIT ocean general circulation model. Adv Atmos Sci 27(3):455–468. https://doi.org/10.1007/s00376-009-9022-6
Isla FI, Toldo EE Jr (2013) ENOS impacts on Atlantic watersheds of South America. Quat Environ Geosci 04(1–2):34–41
Johns W, Lee TN, Schott FA, Zantopp RJ, Evans RH (1990) The North Brazil current retroflection: seasonal structure and eddy variability. J Geophys Res 95(C12):22103–22120. https://doi.org/10.1029/JC095iC12p22103
Kennard MJ, Mackay SJ, Pusey BJ, Olden JD, Marsh N (2010) Quantifying uncertainty in estimation of hydrologic metrics for eco-hydrological studies. River Res Appl 26(2):137–156. https://doi.org/10.1002/rra.1249
Knoppers B, Ekau W, Figueiredo AG (1999) The coast and shelf of east and northeast Brazil and material transport. Geo Mar Lett 19(3):171–178. https://doi.org/10.1007/s003670050106
Kourafalou VH, Oey L, Wang JD, Lee TN (1996) The fate of river discharge on the continental shelf: 1. Modeling the river plume and the inner shelf coastal current. J Geophys Res 101(C2):3415–3434. https://doi.org/10.1029/95JC03024
Lacerda LD, De Araujo DS, Maciel NC (1993) Dry coastal ecosystems of the tropical Brazilian coast. In: van der Maarel (ed) Dry coastal ecosystems: Africa, America, Asia and Oceania. Ecosystems of the world 2B. Elsevier, Amsterdam, pp 477–493
Marengo JA (1992) Interannual variability of surface climate in the Amazon basin. Int J Climatol 12(8):853–863
Marengo JA, Alves LM (2005) Tendências hidrológicas da bacia do rio Paraíba do Sul. Rev Brasil Meteorol 20(2):215–226
Marengo JA, Tomasella J, Uno C (1998) Trends in streamflow and rainfall in tropical South America: Amazonia, eastern Brazil and northwestern Peru. J Geophys Res 103(D2):1775–1783. https://doi.org/10.1029/97JD02551
Marques F (2010) Variabilidade da precipitação na bacia hidrográfica do rio Tubarão/SC de 1946 a 2006. Dissertation, Federal University of Santa Catarina
Martins LR, Coutinho PN (1981) The Brazilian continental margin. Earth Sci Rev 17(1–2):87–107. https://doi.org/10.1016/0012-8252(81)90007-6
Medeiros PRP, Knoppers BA, Dos Santos Junior RC, Souza WFL (2007) Aporte Fluvial e Dispersão de Matéria Particulada em Suspensão na Zona Costeira do Rio São Francisco (SE/AL). Geochimica Brasiliensis 21(2):209–228
MMA (Ministério do Meio Ambiente—Brasil) (2006a) Caderno da Região Hidrográfica do Atlântico Leste/Ministério do Meio Ambiente, Secretaria de Recursos Hídricos. Brasília
MMA (Ministério do Meio Ambiente—Brasil) (2006b) Caderno da Região Hidrográfica do Atlântico Sul/Ministério do Meio Ambiente, Secretaria de Recursos Hídricos. Brasília
Möller OJ, Castaing P, Salomon JC, Lazure P (2001) The influence of local and non-local forcing effects on the subtidal circulation of Patos Lagoon. Estuaries 24(2):297–311. https://doi.org/10.2307/1352953
Nilsson C, Reidy CA, Dynesius M, Revenga C (2005) Fragmentation and flow regulation of the world's large river systems. Science. https://doi.org/10.1126/science.1107887
Oki T (1999) The global water cycle. In: Browning K, Gurney R (eds) Global energy and water cycles. Cambridge University, Cambridge, pp 10–27
Ovalle ARC, Silva CF, Rezende CE, Gatts CEN, Suzuki MS, Figueiredo RO (2013) Long-term trends in hydrochemistry in the Paraíba do Sul River, southeastern Brazil. J Hydrol 481:191–203. https://doi.org/10.1016/j.jhydrol.2012.12.036
Pekárová P, Miklánek P, Pekár J (2006) Long-term trends and runoff fluctuations of European rivers. IAHS-AISH Publication, 308, Wallingford, 520–525
Perry GD, Duffy PB, Miller NL (1996) An extended data set of river discharges for validation of general circulation models. J Geophys Res 101(D16):21339–21349. https://doi.org/10.1029/96JD00932
Razavi T, Coulibaly P (2013) Streamflow prediction in ungauged basins: review of regionalization methods. J Hydrol Eng 18(8):958–975. https://doi.org/10.1061/(ASCE)HE.1943-5584.0000690
Saurral RI, Barros VR, Lettenmaier DP (2008) Land use impact on the Uruguay River discharge. Geophys Res Lett 35:L12401. https://doi.org/10.1029/2008GL033707
Silva ACD, Araujo M, Bourles B (2005) Variação sazonal da estrutura de massas de água na plataforma continental do Amazonas e área oceânica adjacente. Rev Bras Geof 23(2):145–157. https://doi.org/10.1590/S0102-261X2005000200004
Sivapalan M, Takeuchi K, Franks SW, Gupta VK, Karambiri H, Lakshmi V et al (2003) IAHS decade on predictions in ungauged basins (PUB), 2003–2012: shaping an exciting future for the hydrological sciences. Hydrol Sci J 48(6):857–880. https://doi.org/10.1623/hysj.48.6.857.51421
Smoak JM, Patchineelam SR (1999) Sediment mixing and accumulation in a mangrove ecosystem: evidence from 210Pb, 234 Th and 7Be. Mang Salt Marsh 3:17–27
Souza WFL, Medeiros PRP, Brandini N, Knoppers B (2011) Impactos de barragens sobre os fluxos de materiais na interface continente-oceano. Rev Virtual Quim 3(2):116–128. https://doi.org/10.5935/1984-6835.20110016
Taormina R, Chau KW (2015) Data-driven input variable selection for rainfall–runoff modeling using binary-coded particle swarm optimization and Extreme Learning Machines. J Hydrol 529:1617–1632. https://doi.org/10.1016/j.jhydrol.2015.08.022
Trenberth KE, Caron JM, Stepaniak DP (2001a) The atmospheric energy budget and implications for surface fluxes and ocean heat transports. Clim Dyn 17:259–276. https://doi.org/10.1007/PL00007927
Trenberth KE, Stepaniak DP, Hurrell JW, Fiorino M (2001b) Quality of reanalyses in the tropics. J Clim 14:1499–1510
Tucci CEM (2002) Regionalização de Vazões. Editora Universidade, Rio Grande
Vaz AC, Moller OJ, Tabajara LA (2006) Análise quantitativa da descarga dos rios afluentes da Lagoa dos Patos. Atlântica (Rio Grande) 28(1):13–23
Villar JCE, Guyot JL, Ronchail J, Cochonneau G, Filizola N, Fraizy P, Labat D, de Oliveira E, Ordoñez JJ, Vauchel P (2009) Contrasting regional discharge evolutions in the Amazon basin (1974–2004). J Hydrol 375(3):297–311. https://doi.org/10.1016/j.jhydrol.2009.03.004
Wu CL, Chau KW, Fan C (2010) Prediction of rainfall time series using modular artificial neural networks coupled with data-preprocessing techniques. J Hydrol 389:146–167. https://doi.org/10.1016/j.jhydrol.2010.05.040
Zeng N (1999) Seasonal cycle and interannual variability in the Amazon hydrologic cycle. J Geophys Res 104(D8):9097–9106. https://doi.org/10.1029/1998JD200088